Bull. Inst. Chem. Res., Kyoto Univ., Vol. 64, No. 1, 1986

Relativistic Calculations of the Excitation Cross Sections of Hydrogen-Like Ions by Heavy Charged-Particle Impact

Takeshi MUKOYAMA

Received February 4, 1986

The cross sections for excitation from the initial K shell to the final L_1, L_2, and L_3 shells of hydrogen-like ions by heavy charged-particle impact have been calculated using the relativistic wave functions for the target electron in the plane-wave Born approximation. The calculated results are compared with the nonrelativistic calculations and the electronic relativistic effect is discussed.

KEY WORDS: Atomic Excitation/ Electronic Relativistic Effect/ Plane-Wave Born Approximation/

I. INTRODUCTION

The Coulomb excitation of atoms and ions by heavy charged-particle bombardment is of importance in atomic collision and its applications, such as plasma physics and astrophysics. However, this process has so far been much less investigated than the ionization and electron-capture processes in atomic collisions. In addition, almost all existing studies both theoretically and experimentally are limited to the case of excitation of hydrogen or helium by proton and α-particle impact. This is mainly due to experimental difficulties to obtain highly charged ions.

The theoretical calculations for atomic excitation cross sections have been performed in the plane-wave Born approximation (PWBA)[1] and with impact-parameter approach.[2-4] These works are nonrelativistic and useful for targets with low atomic numbers. To the author's knowledge, there has been reported no relativistic calculation for atomic excitation by heavy-particle impact, except for our previous work on the $1s$–$2s$ excitation cross sections.[5]

With recent progress in experimental techniques to produce multiply charged ions, various heavy ions with high charge become available and the collision physics with highly-charged heavy ions is rapidly developing. Considering this fact, it is worthwhile to calculate the atomic excitation cross sections for these heavy ions by the use of relativistic wave functions.

In the present work, the relativistic calculations on the atomic excitation cross sections from the K shell to the L_1, L_2, and L_3 shells of hydrogen-like ions by charged-particle impact have been made in the PWBA. The relativistic hydrogenic (Dirac) wave functions are used for the target electrons, while the projectile is treated nonrelativistically. The relativistic cross sections are compared with the corresponding nonrelativistic ones and the electronic relativistic effect is studied.

* 向山 毅: Laboratory of Nuclear Radiation, Institute for Chemical Research, Kyoto University, Kyoto, 606.

II. THEORY

The fundamental assumptions and general formalism of the PWBA are described in many standard text books on the atomic collision theory. Here we follow the approach of McDowell and Coleman.[6] Throughout the present work, atomic units are used and the excitation cross section is given in units of πa_0^2, where a_0 is the first Bohr orbit of hydrogen.

We assume that the target ion is at rest at the origin of the coordinate. The projectile is treated as a bare nucleus with nuclear charge Z_1 and the atomic number of the target ion is denoted by Z_2. We consider only single-electron excitation process. The cross section for excitation from state i to state f in atomic collision is written by[6]

$$Q=\frac{\mu^2}{2\pi^2}\frac{1}{k_i^2}\int_{p\min}^{p\max}|T_{if}|^2 p\mathrm{d}p, \tag{1}$$

where μ is the reduced mass, $\mathbf{k}_i$ is the initial relative momentum, and $\mathbf{p}$ is the momentum transfer. When the final momentum is expressed as $\mathbf{k}_f$, the maximum and minimum values of $\mathbf{p}$ are given by

$$p_{\min}=|\mathbf{k}_i-\mathbf{k}_f|,$$

and

$$p_{\max}=|\mathbf{k}_i+\mathbf{k}_f|.$$

The matrix element T_{if} is written by

$$T_{if}=<\psi_f(\mathbf{R})\phi_f(\mathbf{r})|V(\mathbf{R},\mathbf{r})|\psi_i(\mathbf{R})\phi_i(\mathbf{r})>, \tag{2}$$

where $\mathbf{R}$ is the position vector of the projectile, $\mathbf{r}$ is that of the target electron, ψ_i and ψ_f are the initial and final wave functions of the projectile, and ϕ_i and ϕ_f are those of the target electron. The interaction potential between the projectile and the target electron is

$$V(\mathbf{R},\mathbf{r})=\frac{Z_1Z_2}{R}-\frac{Z_1}{|\mathbf{R}-\mathbf{r}|}. \tag{3}$$

In the PWBA, the wave functions of the projectile are

$$\psi_i(\mathbf{R})=e^{i\mathbf{k}_i\cdot\mathbf{R}},\ \psi_f(\mathbf{R})=e^{i\mathbf{k}_f\cdot\mathbf{R}}. \tag{4}$$

Substitution of Eq. (4) in Eq. (2) yields

$$T_{if}=Z_1\int\mathrm{d}\mathbf{R}\int\mathrm{d}\mathbf{r}e^{i\mathbf{p}\cdot\mathbf{R}}\phi_f^*(\mathbf{r})\left\{\frac{Z_2}{R}-\frac{1}{|\mathbf{R}-\mathbf{r}|}\right\}\phi_i(\mathbf{r}). \tag{5}$$

The $\mathbf{R}$ integration can be made as usual.[7] Using the orthogonal property of the wave function, Eq. (5) reduces to

$$T_{if}=-\frac{4\pi Z_1}{p^2}\int e^{i\mathbf{p}\cdot\mathbf{r}}\phi_f^*(\mathbf{r})\phi_i(\mathbf{r})\mathrm{d}\mathbf{r}. \tag{6}$$

Inserting Eq. (6) into Eq. (1), the excitation cross section is written as

$$Q=\frac{8Z_1^2}{v^2}\int_{p\min p}^{p_{max}}\frac{1}{3}|\mathcal{I}(p;i\to f)|^2dp, \tag{7}$$

where $v=k_i/\mu$ is the initial velocity of the projectile and

$$\mathcal{I}(p;i\to f)=\int e^{i\mathbf{p}\cdot\mathbf{r}}\phi_f^*(\mathbf{r})\phi_i(\mathbf{r})d\mathbf{r}. \tag{8}$$

The relativistic hydrogenic wave functions are given by[8]

$$\phi(\mathbf{r})=\begin{pmatrix} g_\kappa(r)\ \chi_\kappa^\mu(\hat{r}) \\ if_\kappa(r)\ \chi_{-\kappa}^\mu(\hat{r}) \end{pmatrix}, \tag{9}$$

where κ is the relativistic quantum number, μ is the magnetic quantum number, $\chi_\kappa^\mu(\hat{r})$ is the spin-angular momentum part of the wave function, and $\hat{r}$ is the unit vector of the direction of $\mathbf{r}$. The large and small components of the radial wave function are

$$g_k(r)=N(1+W)^{1/2}(c_0+c_1r)r^{\gamma-1}e^{-\lambda r}, \tag{10a}$$

and

$$f_k(r)=-N(1-W)^{1/2}(a_0+a_1r)r^{\gamma-1}e^{-\lambda r}. \tag{10b}$$

The parameters, N, W, a_0, a_1, c_0, c_1, γ, and λ, are defined in Ref. 8 for K, L_1, L_2, and L_3 shells.

By the use of the wave functions in Eq. (10), the relativistic matrix elements are

$$\mathcal{I}(p;\mathrm{K}-\mathrm{L}_1)=G_0(p), \tag{11}$$

$$\mathcal{I}(p;\mathrm{K}-\mathrm{L}_2)=(4\pi)^{1/2}\mathrm{C}(1/2\,1\,1/2;\,\mu_1\,\mu_2-\mu_1)Y^*_{1\,\mu_2-\mu_1}(\hat{p})G_1(p), \tag{12}$$

$$\mathcal{I}(p;\mathrm{K}-\mathrm{L}_3)=(4\pi)^{1/2}\mathrm{C}(1/2\,1\,3/2;\,\mu_1\,\mu_2-\mu_1)Y^*_{1\,\mu_2-\mu_1}(\hat{p})G_1(p), \tag{13}$$

where

$$G_L(p)=N_1N_2[(c_0W_+ + a_0W_-)I_0^{(L)}+(c_1W_+ + a_1W_-)I_1^{(L)}], \tag{14}$$

$$W_+=[(1+W_1)(1+W_2)]^{1/2},$$
$$W_-=[(1-W_1)(1-W_2)]^{1/2},$$
$$I_i^{(L)}=\int_0^\infty e^{-(\lambda_1+\lambda_2)r}j_L(pr)r^{\gamma_1+\gamma_2+i}dr, \tag{15}$$

$\mathrm{C}(a,\,b,\,c;\,d,\,e)$ is the Clebsch-Gordan coefficient, $Y_{lm}(\hat{p})$ is the spherical harmonics, $\hat{p}$ is the unit vector in the direction of $\mathbf{p}$, and $j_L(x)$ is the spherical Bessel function of order L. The parameters, N_1, W_1, γ_1, and λ_1 correspond to those for the K-shell electron, while N_2, W_2, γ_2, λ_2, a_0, a_1, c_0, and c_1 are the parameters for L_j-shell electron ($j=1$–3).

The radial integral $I_i^{(L)}(p)$ [Eq. (15)] is obtained analytically using the definition of the spherical Bessel function and the integration formula.[9] The final expression is given by

$$\int_0^\infty e^{-ax}j_l(bx)x^\mu dx=\left(\frac{\pi}{2b}\right)^{1/2}\frac{b^{l+1/2}\Gamma(l+\mu+1)}{2^{l+1/2}a^{l+\mu+1}\Gamma(l+3/2)}$$
$$\times{}_2F_1\left(\frac{l+\mu+1}{2},\ \frac{l+\mu+2}{2};\ l+3/2;\ -\frac{b^2}{a^2}\right), \tag{16}$$

where ${}_2F_1(a, b; c; x)$ is the Gauss-type hypergeometric function.

Letting $\gamma=|\kappa|$ for the initial and final states, Eqs. (11), (12), and (13) reduce to the corresponding nonrelativistic limits. These results are equivalent to the nonrelativistic expressions of Bates and Griffing:[1]

$$\mathcal{I}|(p;\ 1s\to 2s)|=2^{17/2}\,Z_2^2p^2/(9Z_2^2+4p^2)^3, \tag{17}$$

and

$$\mathcal{I}|(p;\ 1s\to 2p)|=3\ 2^{15/2}\,Z_2^5p/(9Z_2^2+4p^2)^3. \tag{18}$$

III. RESULTS AND DISCUSSION

We have performed the PWBA calculations for the K—L_1, K—L_2, and K—L_3 excitation cross sections using the relativistic and nonrelativistic hydrogenic wave functions for the target electrons. The projectile is considered as a bare nucleus and the target is a hydrogen-like ion. In the nonrelativistic case, the LS-coupled wave functions are used for the L_2- and L_3-shell electrons in the target ion. All the numerical calculations in the present work have been made on the FACOM M-382 computer in the Data Processing Center of Kyoto University.

In Fig. 1, the relativistic and nonrelativistic cross sections of the K—L_1 excitation for protons on Fe^{25+} ion are plotted as a function of proton energy. These results are

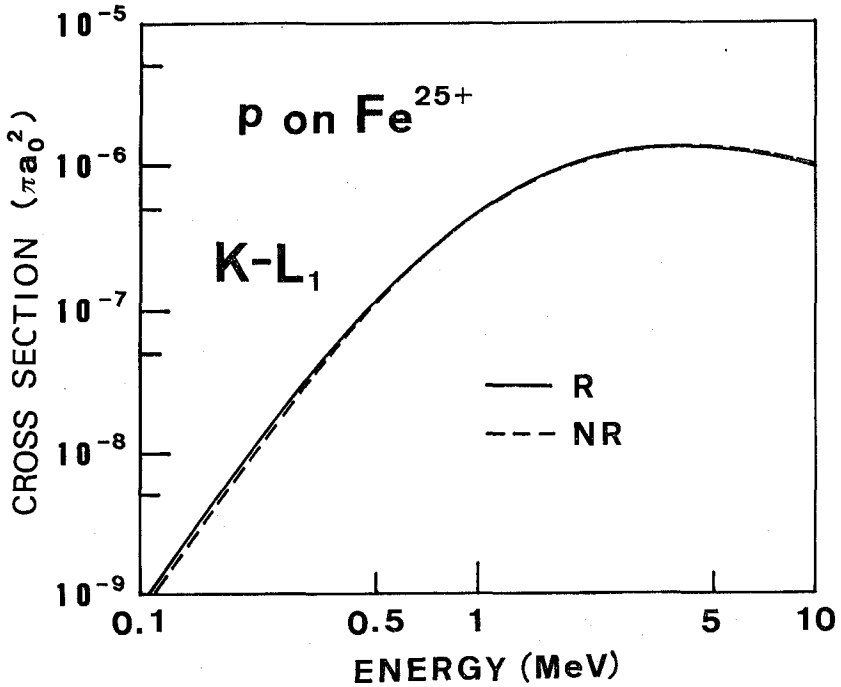

Fig. 1. Cross sections for K-L_1 excitation of Fe^{25+} ion by proton impact. The solid curve represents the relativistic cross sections and the dashed curve indicates the nonrelativistic ones.

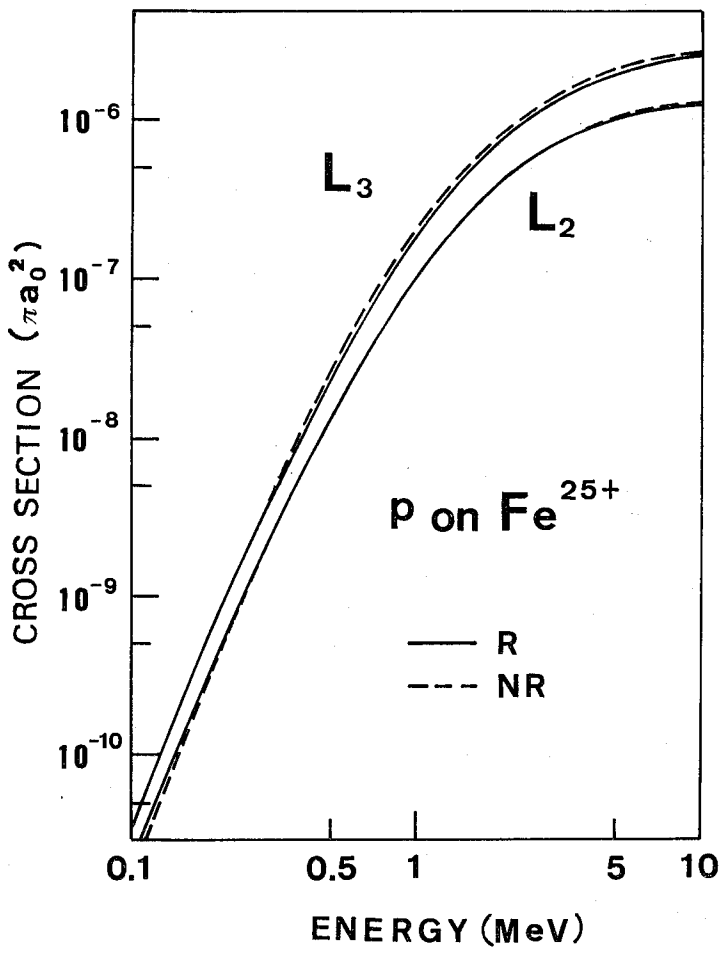

Fig. 2. Cross sections for K-L_2 and K-L_3 excitation of Fe^{25+} ion by proton impact. See caption of Fig. 1.

in good agreement with the values obtained from the impact-parameter method with straight-line trajectory.[5] For low energies, the relativistic cross sections are slightly larger than the nonrelativistic ones, but in the high-energy region the nonrelativistic values become larger. The relativistic PWBA cross sections of the K—L_1 excitation of Sn^{49+} and U^{91+} ions by proton impact were also calculated and found to agree well with the results of the previous work in the impact-parameter approach.[5]

Figure 2 shows comparison of the relativistic and nonrelativistic PWBA cross sections of the K—L_2 and K—L_3 excitation for protons on Fe^{25+} ion. For these cases, the relativistic cross sections are larger than the nonrelativistic ones in low-energy region and smaller at high energies. The relativistic effect is larger for L_3 shell than for L_2 shell. The K—L_2 and K—L_3 excitation cross sections for proton impact on Sn^{49+} ion are plotted in Fig. 3 as a function of proton energy. Although the relativistic effect is somewhat enhanced, the general trend of the cross sections as a function of energy is similar to that for Fe^{25+} ion.

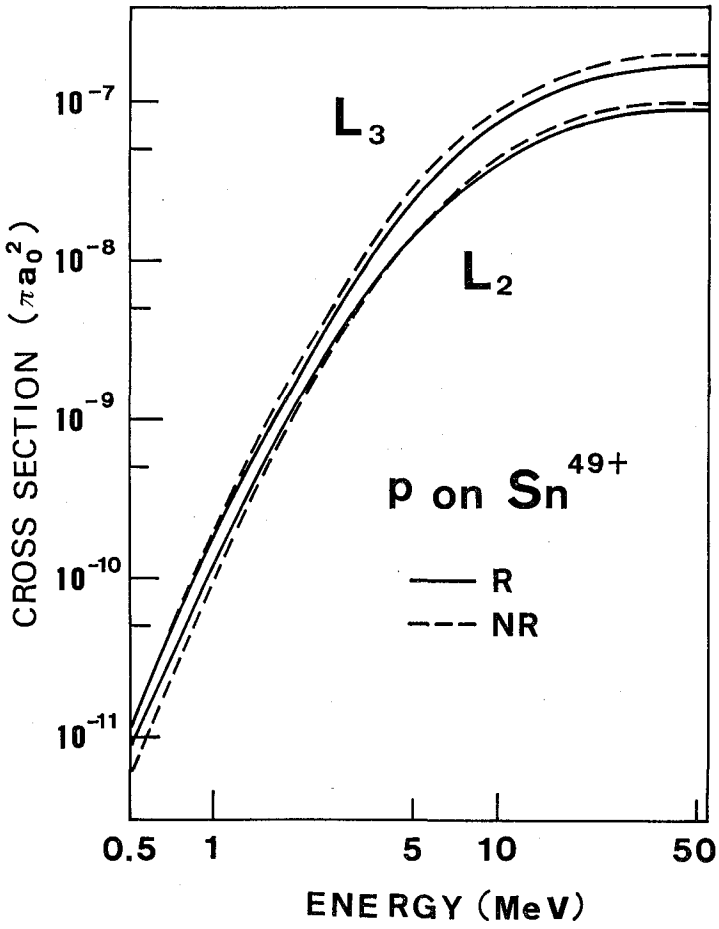

Fig. 3. Cross sections for K-L_2 and K-L_3 excitation of Sn^{49+} ion by proton impact. See caption of Fig. 1.

Figure 4 demonstrates the relativistic effect in the K—L_2 and K—L_3 excitation cross sections for protons on U^{91+} ion. At 1 Mev, the relativistic K—L_2 excitation cross section is approximately 7 times larger than the nonrelativistic one. With increasing energy the relativistic curve approaches to the nonrelativistic line and then becomes lower than the latter. For the energy of 100 MeV, the relativistic value is about 1.5 times smaller. The relativistic K—L_3 cross section is slightly larger than the nonrelativistic value in low-energy region and becomes smaller for the energy region above 2 MeV. At 100 MeV the former value is about one half of the latter and nearly equal to the nonrelativistic value for the K—L_2 excitation.

The K–L excitation cross sections of U^{91+} ion by $^{12}C^{6+}$-ion impact are shown in Fig. 5. The energy scale is expressed as the projectile energy divided by its mass. In this case, the universal property of the cross section for projectile mass and charge does not hold because of the definition of p_{min}.

In conclusion, we have calculated the relativistic PWBA cross sections of hydrogen-

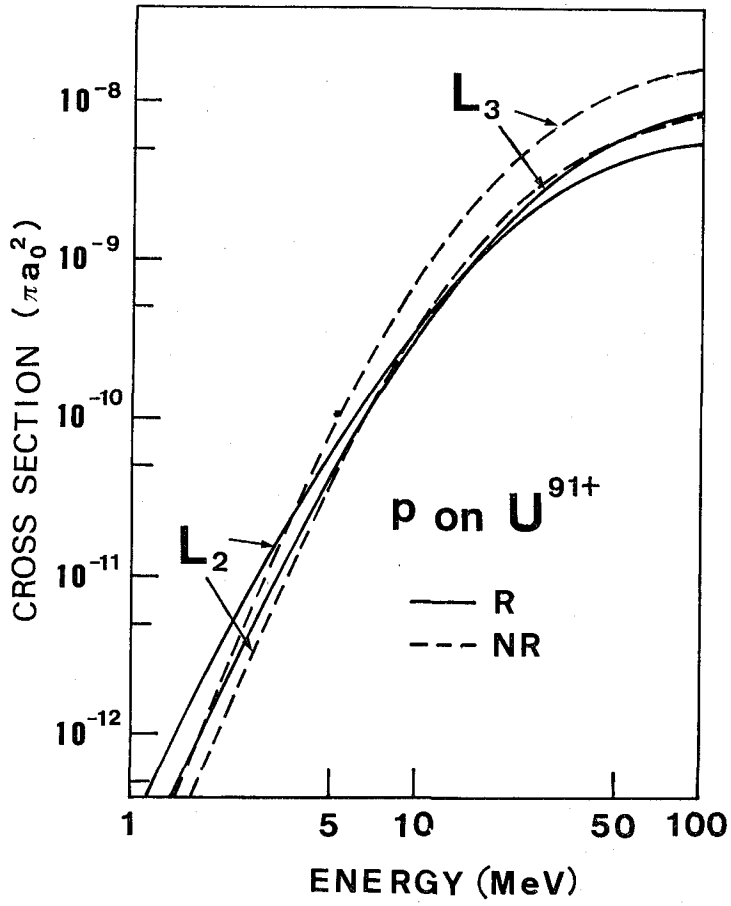

Fig. 4. Cross sections for K-L_2 and K-L_3 excitation of U^{91+} ion by proton impact. See caption of Fig. 1.

like ions by heavy charged-particle impact for K—L_1, K—L_2, and K—L_3 excitation. It is found that in low-energy region the relativistic effect increases the cross section, but decreases it for high-energy projectiles.

The relativistic effect can be ascribed to two reasons, the relativistic wave functions and the relativistic binding energies. The use of the relativistic wave functions increases the excitation cross section in all cases studied here. The enhancement of the cross section is large for low energies and small at high energies. On the other hand, the relativistic binding energies decrease the cross section.

In the low-energy region the enhancement due to the wave-function effect surpasses the reduction due to the use of the relativistic binding energies and the relativistic cross section is larger than the nonrelativistic one. On the contrary, the situation is reversed for high energies and the relativistic cross section becomes smaller the nonrelativistic cross section.

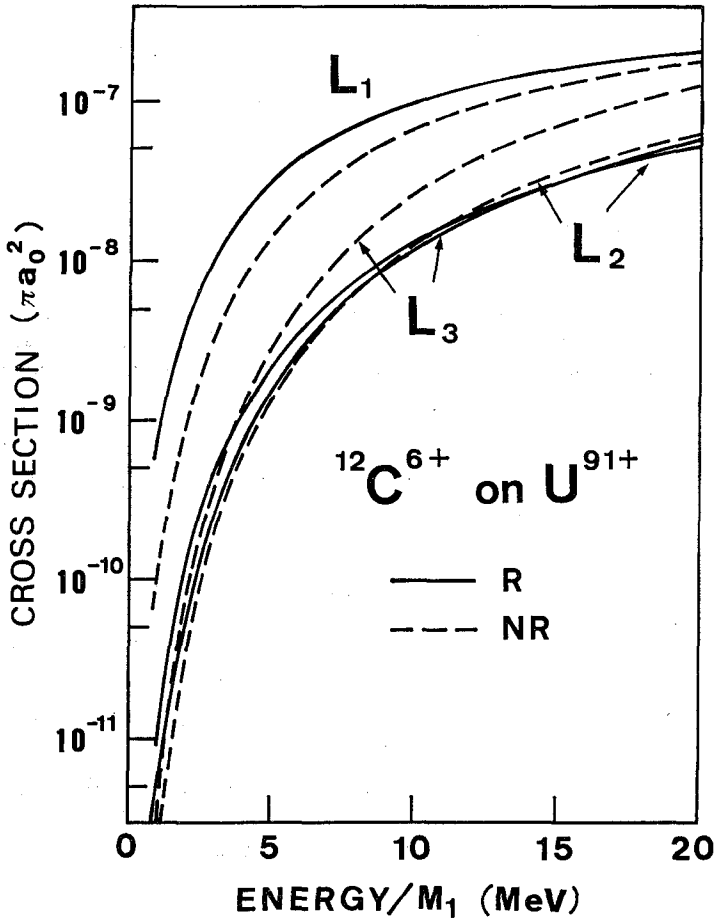

Fig. 5. Cross sections for K-L_1, K-L_2, and K-L_3 excitation of U^{91+} ion by $^{12}C^{6+}$-ion impact. See caption of Fig. 1.

REFERENCES

(1) D. R. Bates and G. Griffing, *Proc. Phys. Soc.* (*London*), **66**, 961 (1953).
(2) D. R. Bates, *Proc. Roy. Soc.* (*London*) *A*, **245**, 299 (1958).
(3) J. Van den Bos and F. J. De Heer, *Physica*, **34**, 333 (1967).
(4) D. R. Bates and R. J. Tweed, *J. Phys. B*, **7**, 117 (1974).
(5) T. Mukoyama, *Bull. Inst. Chem. Res., Kyoto Univ.*, **63**, 16 (1985).
(6) M. R. C. McDowell and J. P. Coleman, "Introduction to the Theory of Ion-Atom Collisions," North-Holland, Amsterdam, (1970).
(7) H. Bethe, *Ann. Physik*, **5**, 325 (1930).
(8) M. E. Rose, "Relativistic Electron Theory," Wiley, New York, (1961).
(9) W. Magnus, F. Oberhettinger, and R. P. Soni, "Formulas and Theorems for the Special Functions of Mathematical Physics," Springer, Berlin, (1966).